

Raman lidar measurements of aerosol distribution and cloud properties

Sachin J. Verghese, Adam H. Willitsford and C. Russell Philbrick
Department of Electrical Engineering, The Pennsylvania State University
University Park, PA 16802

ABSTRACT

Measurements obtained by the PSU Lidar Atmospheric Profile Sensor (LAPS) Raman lidar, during different periods, provide a comprehensive dataset to characterize cloud properties and aerosol distributions. The PSU Raman lidar measures the profiles of molecular nitrogen, molecular oxygen and the rotational Raman scatter (the mixture of all molecular species) at both visible and ultraviolet wavelengths, which are then used to generate vertical aerosol extinction profiles from the incremental extinction. Since the optical extinction at different wavelengths is strongly dependent on the size distribution of aerosols, variations in the profile of the size distribution can be inferred over an interesting range corresponding to accumulation mode particles, 50 nm to 1 μ m. The variation in the extinction profiles at different wavelengths is also used along with the water vapor profiles to observe the formation, growth and dissipation of cloud structures. The water vapor concentrations have been seen to decrease in regions surrounding a growing cloud as the particles increase in size by absorbing the water. Also, the water vapor concentration is found to increase as clouds begin to dissipate. The change in the size of the cloud particles during the different stages can also be observed in the multi-wavelength aerosol extinction. Results obtained from different locations, and for a wide range of atmospheric conditions, are used to compare and contrast the aerosol distributions and also to study the physical properties of clouds.

Keywords: Raman lidar, remote sensing, optical extinction, aerosol distribution, cloud physics.

1. INTRODUCTION

Aerosols play vital roles in balancing the Earth's radiation budget, in applications of electro-optic sensors, and they are of increasing importance due to their impact on human health from air pollution. Atmospheric aerosols are generated from various natural and anthropogenic sources and include all liquid and solid particles, except pure water, that exist in the atmosphere under normal conditions¹. Studies have shown tropospheric aerosols to be directly related to a myriad of health problems². Particles having a diameter less than 2.5 microns, referred to as PM_{2.5}, are considered to be of greater risk to human health because a large number of these particles are associated with the emissions from combustion products and carry carcinogenic materials. Particles having a diameter less than 10 microns (PM₁₀) are also considered to be a risk to human health but this older standard appears to be less descriptive of their pollution hazard. The distribution of aerosols in the atmosphere influences Earth's climate because the scattering and absorption by particles, those in aerosols and clouds, play a major role in determining what fraction of the solar radiation incident at the top of the atmosphere reaches the Earth's surface. The propagation of light through the atmosphere is also strongly affected by the presence of aerosols, and hence causes a significant deterioration in the performance of electro-optic sensors. In order to mitigate the effects of aerosols, research efforts are focused on identifying and predicting production and transport mechanisms as well as ascertaining number densities and species concentrations. Raman lidar provides one of the best techniques for describing the aerosol distributions and studying cloud properties. Because the gradient of the vertical profile of the primary constituents is well known, the difference in the slope of the measured profile from the molecular scale height can be used to determine the incremental extinction and thereby generate an aerosol extinction profile. By taking the ratio of extinction at three different wavelengths we can describe changes in particle size and density as a function of time and altitude.

2. LAPS RAMAN LIDAR INSTRUMENT

The Lidar Atmospheric Profile Sensor (LAPS) instrument was built by the staff and graduate students of the Applied Research Laboratory and the Electrical Engineering Department of Penn State University for the U.S Navy. It

was the fifth Raman lidar developed by the group since 1978 and was the first prototype prepared as an operational Raman lidar. The LAPS instrument uses Raman lidar techniques to simultaneously provide profiles of water vapor, temperature, ozone and optical extinction³. The LAPS lidar consists of more than twenty sub-systems to control its operation and obtain measurements. The main components of the LAPS system are summarized in Table 1. LAPS was first tested onboard a U.S. Navy ship, the USNS SUMNER during September and October 1996 in the Gulf of Mexico and Atlantic Ocean. Since then it has been used in a number of research investigations, which have provided a large dataset that will now be used for investigations of aerosol and cloud properties. PSU's LAPS Raman lidar is a rugged instrument and was designed for automatic operation to enable measuring in virtually any environment at any given time.

The Raman scattering technique is advantageous because of its rugged and rigorous quantitative measurement capabilities using a single transmitted wavelength. Raman scatter signals can be used to identify a trace constituent and quantify it relative to the major constituents of a mixture⁴. Measurements of the atmospheric properties are obtained from the return signal intensity at the transmitted wavelength as well as at Raman shifted wavelengths. The LAPS instrument uses the vibrational Raman scattered signals to measure water vapor, ozone and optical extinction, and uses the rotational Raman scatter signals to measure temperature. It collects the rotational Raman backscatter signals at 528 nm and 530 nm and the vibrational Raman backscatter signals at 607 nm, 660 nm, 277 nm, 284 nm and 295 nm. The 607 nm and 660 nm signals are the 1st Stokes vibrational Raman shifts from the N₂ and H₂O molecules in the atmosphere excited by the second harmonic (532 nm) of the Nd:YAG laser. The 277 nm, 284 nm and 295 nm signals correspond to the 1st Stokes vibrational Raman shifts from the O₂, N₂, and H₂O molecules in the atmosphere excited by the fourth harmonic (266 nm) of the Nd:YAG laser. The measurement capabilities of the LAPS instrument using Raman scatter techniques are summarized in Table 2. The optical extinction and water vapor measurement techniques are described below.

Table 1 Summary of LAPS subsystems.

Transmitter	Continuum 9030 –30 Hz 5X Beam Expander	600 mJ @ 532 nm 130 mJ @ 266 nm
Receiver	61 cm Diameter Telescope	Fiber optic transfer
Detector	Eight PMT channels Photon Counting	660 and 607 nm – Water Vapor 528 and 530 nm – Temperature 295 and 284 nm – Daytime Water Vapor 277 and 284 nm – Raman/DIAL Ozone 607, 530, and 284 nm – Extinction 532 nm – Backscatter
Data System	DSP 100 MHz	75-meter range bins
Safety Radar	Marine R-70 X-Band	Protects 6° cone angle around beam

Table 2. Measurement capabilities of the LAPS system.

Property	Measurement	Altitude (km)	Time Resolution
Water Vapor	660/607 Raman 295/284 Raman	Surface to 5 Surface to 3	Night - 1 min. Day/Night - 1 min.
Temperature	528/530 Rotational Raman	Surface to 5	Night - 30 min.
Optical Extinction - 530 nm	530 nm Rotational Raman	Surface to 5	Night 10 to 30 min.
Optical Extinction - 607 nm	607 nm Vibrational Raman	Surface to 5	Night 10 to 30 min.
Optical Extinction - 284 nm	284 nm Vibrational Raman	Surface to 3	Day/Night 30 min.
Ozone	277/285 Raman/DIAL	Surface to 3	Day/Night 30 min.

Optical extinction, which is a measure of the total attenuation of a laser beam due to scattering and absorption in the atmosphere, is obtained directly from the slope of the molecular profiles compared to their expected hydrostatic gradient. The LAPS instrument measures the optical extinction profiles from the gradients in each of the measured molecular profiles, at 607 nm, 530 nm and 284 nm. For these wavelengths the extinction is mainly from optical scattering due to airborne particulate matter. The extinction coefficient can be derived directly from the Raman lidar equation⁵. The Raman lidar equation can be written as,

$$P(\lambda_R, z) = E_T(\lambda_T) \xi_T(\lambda_T) \xi_R(\lambda_R) \frac{c\tau}{2} \frac{A}{z^2} \beta(\lambda_T, \lambda_R) \exp \left[- \int_0^z [\alpha(\lambda_T, z') + \alpha(\lambda_R, z')] dz' \right] \quad (1)$$

where z is the altitude of the scattering volume element, λ_T is the wavelength transmitted, λ_R is the wavelength received, $E_T(\lambda_T)$ is the light energy per laser pulse transmitted at wavelength λ_T , $\xi_T(\lambda_T)$ is the net optical efficiency of all transmitting devices at wavelength λ_T , $\xi_R(\lambda_R)$ is the net optical efficiency of each receiving device at wavelength λ_R , c is the speed of light, τ is the time duration of the laser pulse, A is the area of the receiving telescope, $\beta(\lambda_T, \lambda_R)$ is the back scattering cross section of the volume element for the laser wavelength λ_T at Raman shifted wavelength λ_R , and $\alpha(\lambda, z')$ is the extinction coefficient at wavelength λ at range z' . The extinction coefficients in (1) can be written as,

$$\alpha(\lambda_T, z) + \alpha(\lambda_R, z) = \alpha_{\lambda_T}^{mol-sca}(z) + \alpha_{\lambda_T}^{aer-sca}(z) + \alpha_{\lambda_R}^{mol-sca}(z) + \alpha_{\lambda_R}^{aer-sca}(z) + \alpha_{\lambda_T}^{abs}(z) + \alpha_{\lambda_R}^{abs}(z) \quad (2)$$

where $\alpha_{\lambda}^{mol-sca}(z)$ and $\alpha_{\lambda}^{aer-sca}(z)$ are the extinction coefficients due to molecular and aerosol scattering at the transmit and receive wavelengths, and α_{λ}^{abs} are the molecular and aerosol extinction coefficients due to optical absorption. The molecular scattering contribution to the extinction can be easily taken into account. The selected visible wavelengths do not correspond to molecular absorption features in the atmosphere, and the only molecular absorption of significance in the ultraviolet is ozone. The aerosol profile measurements of extinction include aerosol scatter and aerosol absorption contribution. The aerosol extinction coefficient at the visible wavelengths can be expressed by rewriting (1) as,

$$\alpha_{\lambda_R}^{aer} = \frac{\frac{d}{dz} \left[\ln \frac{N(z)}{P(z)z^2} \right] - \alpha_{\lambda_T}^{mol}(z) - \alpha_{\lambda_R}^{mol}(z)}{1 + \frac{\lambda_T}{\lambda_R}} \quad (3)$$

For the UV wavelength the absorption is significant due to ozone absorption and hence the extinction equation includes the compensation for the ozone absorption as given below,

$$\alpha_{\lambda_R}^{aer} = \frac{\frac{d}{dz} \left[\ln \frac{N(z)}{P(z)z^2} \right] - \alpha_{\lambda_T}^{mol}(z) - \alpha_{\lambda_R}^{mol}(z) - \alpha_{\lambda_T}^{Abs}(z) - \alpha_{\lambda_R}^{Abs}(z)}{1 + \frac{\lambda_T}{\lambda_R}} \quad (4)$$

Water vapor concentration is a fundamental property of the atmosphere and provides us with information about some of the most important properties of our environment. The earliest Raman lidar measurements to yield the spatial distribution of water vapor in the atmosphere were performed by Melfi and Cooney^{6, 7}. They used a frequency-doubled Q-switch ruby laser and normalized their water vapor return using the nitrogen vibrational Raman return. The LAPS instrument measures the water vapor mixing ratio by taking the ratio of the signals from the 1st Stokes vibrational Raman shifts for water vapor and nitrogen. Profiles of water vapor can be obtained during the day (295/284) and the night (660/607) with the ultraviolet and visible laser wavelengths. LAPS has the capability of obtaining day time measurements by operating in the 'solar blind' spectral interval, between 230 nm and 300 nm, where stratospheric ozone absorbs the incoming radiation and limits the strong sky background radiance. The water vapor mixing ratio is

expressed by taking the ratio of its number density to the number density of ambient air and multiplying by a calibration constant. The equation to obtain vertical profiles of water vapor at visible wavelengths is,

$$W(z) = K_{cal} \frac{S_{H2O}}{S_{N2}} \quad [5]$$

where,

- S_{H2O} is the received signal from the vibrational Raman shift of H₂O at 660 nm,
- S_{N2} is the received signal from the vibrational Raman shift of N₂ at 607 nm,
- K_{cal} is a calibration constant.

The calibration constant, K_{cal} , is obtained by fitting the ratio of the return signals of H₂O and N₂ with the data obtained from radiosondes balloons for water vapor at the same time. Since we are taking the ratio of the two signals and the numerator and the denominator have the same transmit wavelength most of the terms in the lidar equation cancel providing a simpler equation⁸.

3. RESULTS

The LAPS lidar has a distinct advantage in being able to measure optical extinction at different wavelengths and we use this to infer particle size variation by taking ratios of the extinction coefficients at the different wavelengths. Fig. 1 shows a model calculation of the ratios of the extinction coefficients of 530 nm/284 nm and 607 nm/530 nm. The calculation was done assuming only spherical particles using Mie theory. We see that the ratios of the extinction coefficients provide us with information about variations in the size of particles. When the particle size is small compared to wavelength, the scattered intensity follows Rayleigh's theory and is inversely proportional to the fourth power of the wavelength while the scatter cross-section increases as the sixth power of radius. For accumulation mode particles, where the size range is from 0.05 μm to 1 μm, the ratios of the extinction coefficients are size dependent. For coarse mode particles the ratios lose their size dependence and approach unity.

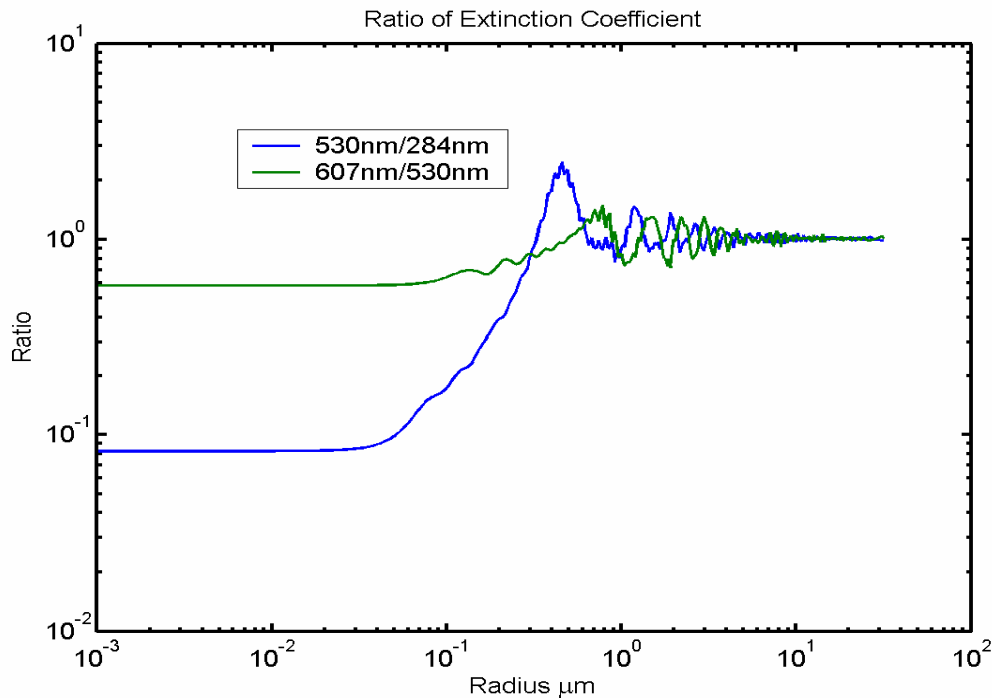


Figure 1: Ratios of extinction coefficients as a function of particle size calculated using Mie theory.

Fig. 2 shows an example of the optical extinction measurements made at the three wavelengths during the SCOS97 measurement program. The vertical profiles show the variation of extinction with altitude. By comparing with the model calculations we observe that large particles seem to dominate in the lower atmosphere, from the surface at 1.2 km up to about 1.7 km, as the UV and visible extinction coefficients imply the presence of accumulation mode particles with sizes near the wavelengths of visible light. At higher altitudes, between 1.7 km and 4 km, the ultraviolet extinction is much greater than the visible extinction and this suggests a distribution of smaller particles in this region (refer to Fig. 1). We also observe two layers with no significant wavelength dependence above 4.5 km where the scattering is due to large particles in a cloud.

Extinction Profiles 09/17/97 04:00-04:59 PDT Hesperia, CA

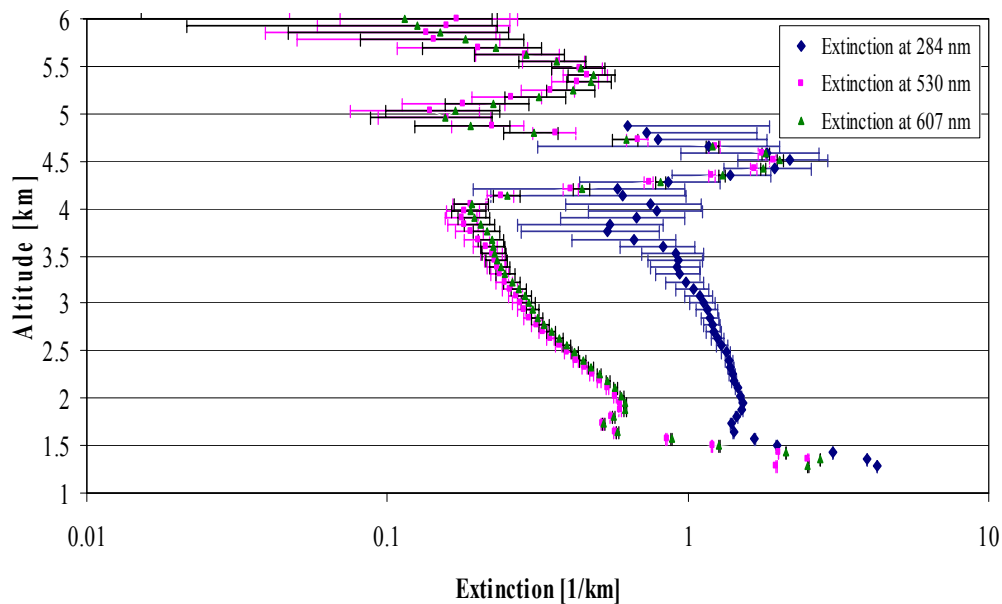


Figure 2: One-hour integrated vertical profiles of optical extinction at 284 nm, 530 nm and 607 nm on September 17, 1997.

Fig. 3(a) and 3(b) show the time sequence plots of extinction at the ultraviolet and visible wavelengths on the night of August 16, 1999 at Philadelphia during the NARSTO-NEOPS campaign. The two plots are aligned with each other so that the overlapping time period in both plots can be better visualized. During this time period we see several aerosol cloud layers advect through the laser beam and the analysis of the ratio of the extinction coefficient of 530nm/284nm shows the results relative to particle size variations in regions inside and surrounding the cloud layers. The ratio of the extinction coefficients for different times, as the clouds pass through the laser beam, is shown in Fig. 4. The different periods of integration in Fig. 4 are shown with similar colored lines in Fig. 3. We see in Fig. 3(a) and 3(b) the presence of a cloud at 0045 UTC and we see the expected increase in the extinction coefficient ratios in Fig. 4. The ratio is very close to 1 inside the cloud and this suggests that the cloud is formed by relatively large size particles ($>1\mu\text{m}$). The ratio of 530 nm to 284 nm is also higher near the ground and this indicates a higher concentration of larger aerosol particles at the surface layer. The ratio of the extinction coefficients at the different times, as shown in Fig. 4, also depicts the evolution of the cloud in terms of particle size variations. Comparing the time sequences with the ratio plot we see that as the cloud begins to dissipate the ratio begins to fall to lower values, which follows the expectation due to the decrease in cloud particle sizes. We can also infer a slight increase in particle sizes from 1 km to 1.4 km in Fig.4, and this growth of particles is evident in the time sequences plots as a corresponding increase in extinction in that region. Comparing with the model calculation of the ratios, the size difference between the top and bottom of the 1 km

and 1.4 km region is about 150 nm. Also, the particle size change at 1.4 km between 0045 UTC and 0125 UTC is seen to be about 70 nm. Fig. 3 is also important because it shows the capability of the LAPS Raman lidar to look through dense clouds. This is advantageous because it enables us to study the top and bottom layers of various cloud and aerosol layers.

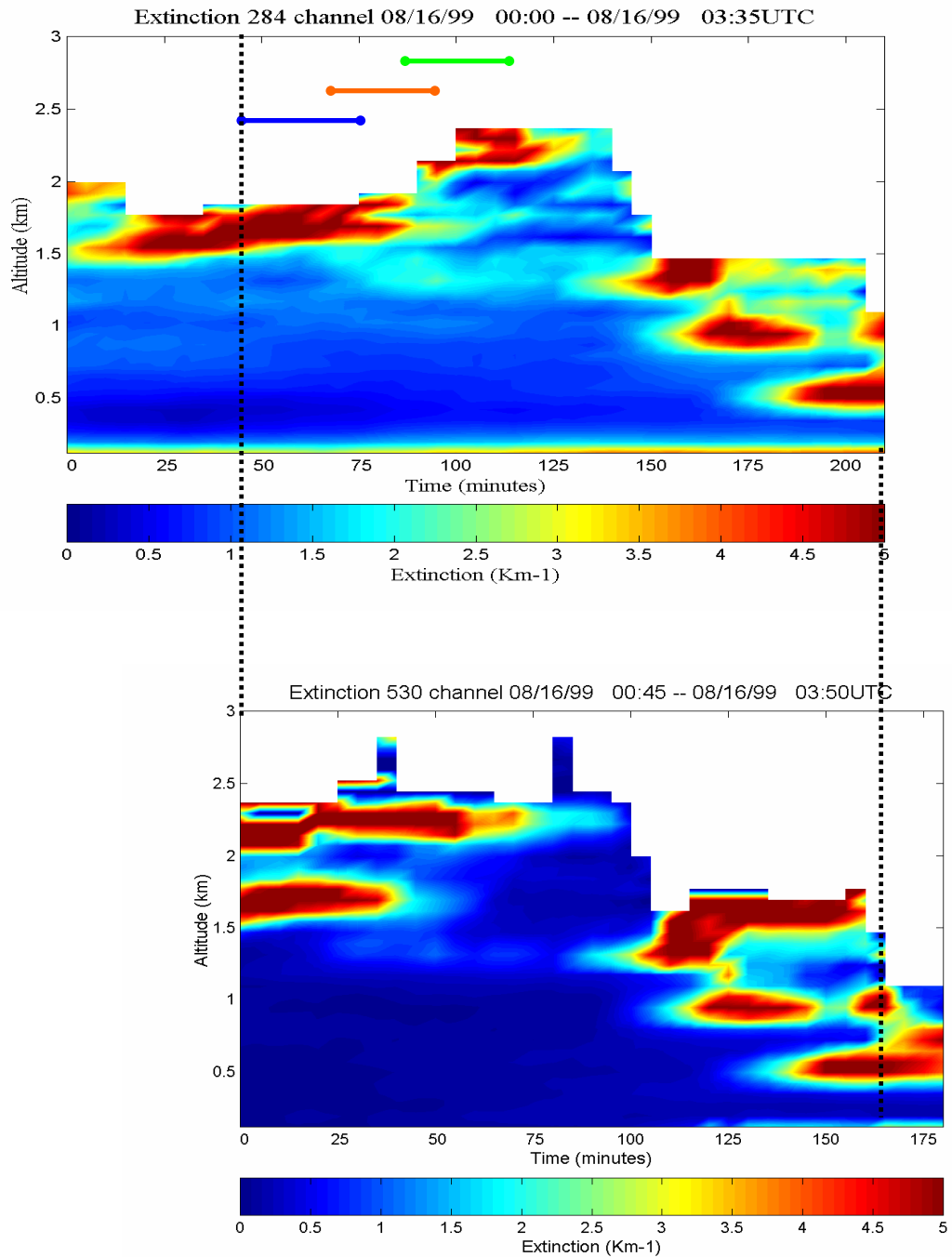


Figure 3: Time sequence plot of extinction on August 16, 1999 (a) at 284 nm (b) at 530 nm.

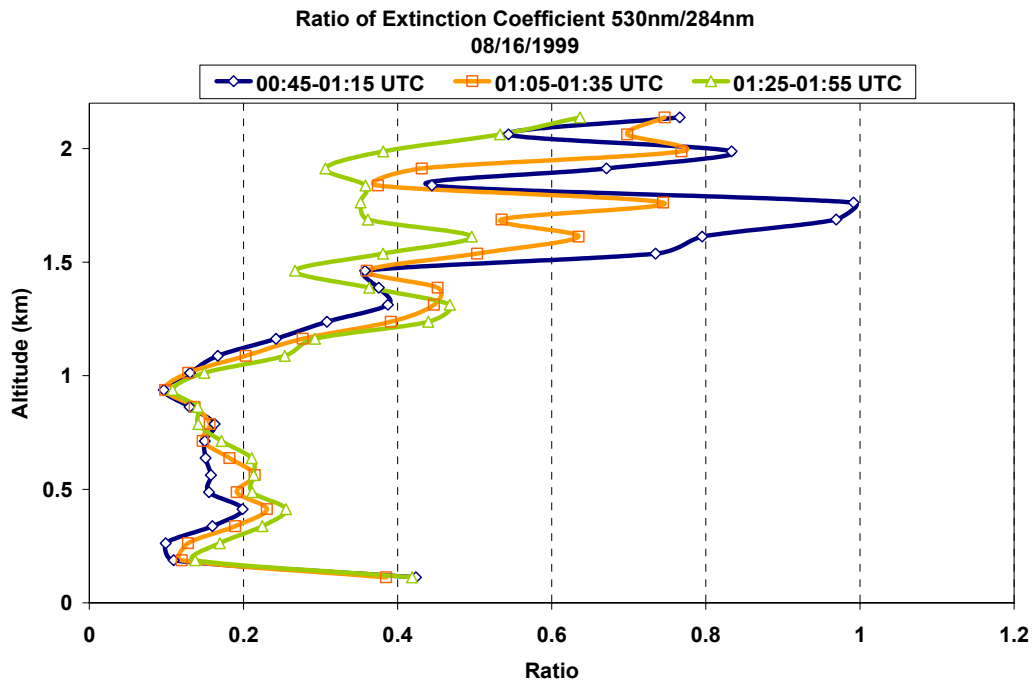


Figure 4: Ratio of extinction coefficient of 530 nm to 284 nm on August 16, 1999.

The variation in the extinction profiles at different wavelengths is also used along with the water vapor profiles to observe the formation, growth and dissipation of cloud structures. The water vapor concentrations have been seen to decrease in regions surrounding a growing cloud as the particles grow in size by absorbing the water. Also, the water vapor concentrations are found to increase as the cloud begins to dissipate. Fig. 5 shows the time sequence plots of extinction and water vapor mixing ratio measured using the LAPS Raman lidar during the SCOS97 campaign. We see the presence of a growing cloud in the extinction measurements at around 2100 UTC. The water vapor measurements show high water vapor mixing ratio values in the region of the cloud and lower values in regions surrounding the cloud. The reduced water vapor mixing ratio values surrounding the cloud is attributed to the absorption of water by the aerosols to form the cloud. As the particles begin to grow they start to absorb excess water from the surrounding regions. Conversely, we have observed in a number of data sets that a dissipating cloud is characterized by a region surrounded by excess water vapor.

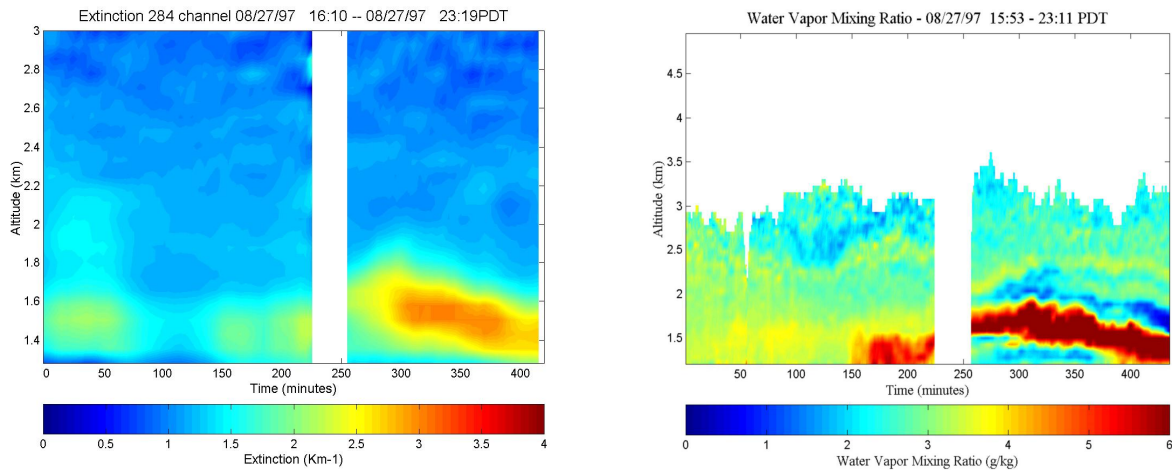


Figure 5: Time sequence plots of optical extinction and water vapor mixing ratio on August 27, 1997.

4. CONCLUSIONS

Raman lidar techniques provide a direct measure of aerosol and cloud properties by simultaneously measuring optical extinction profiles at several different wavelengths. The variations in aerosol size distribution can be described based upon the ratio of the extinction coefficients at the different wavelengths. The ratio of the extinction coefficients is seen to be size dependent for accumulation mode particles, with size range from 50 nm to 1 μm , and size independent for larger particles. We see that the analysis of the ratios provide a means to determine changes in the size distribution of aerosols in the atmosphere and also to describe formation processes in cloud layers. The multi-wavelength extinction profiles are also used along with the water vapor profiles to observe the evolution of cloud structures. Water vapor concentrations have been seen to decrease in regions surrounding a growing cloud and increase as the cloud begins to dissipate. A combination of the above techniques will be used in the future to investigate microphysical properties of clouds using data that has been collected in the several measurement campaigns.

ACKNOWLEDGMENT

These research investigations, the PSU lidar development, shipboard testing, and field investigations have been supported by the following organizations: US Navy through SPAWAR Systems Division - San Diego, PMW-185, NAVOCEANO, NAWC Point Mugu, ONR, DOE, EPA (R826373), CARB, NASA and NSF. The NE-OPS research investigations have been supported by the Pennsylvania DEP and the USEPA STAR Grants Program #R826373. The efforts of Richard Clark and Bruce Doddridge are gratefully acknowledged. The hardware and software development has been possible because of the talents of several engineers and technicians at the PSU Applied Research Laboratory and the graduate students of the Department of Electrical Engineering. Special appreciation goes to D.B. Lysak, T.M. Petach, T.D. Stevens, P.A.T. Haris, M. O'Brien, S.T. Esposito, K. Mulik, A. Achey, E. Novitsky, and H. Li for outstanding contributions.

REFERENCES

1. Arya, S. Pal, Air Pollution Meteorology and Dispersion, Oxford University Press, Oxford, 1999.
2. Hidy, G. M., P. M. Roth, J. M. Hales and R. Scheffe, Oxidant Pollution And Fine Particles: Issues And Needs. *NARSTO Critical Review Series*, 1998.
3. Philbrick, C.R., "Overview of Raman Lidar Techniques for Air Pollution Measurements," Lidar Remote Sensing for Industry and Environment Monitoring II, SPIE Vol. 4484, 136 - 150, 2001.
4. Measures, Raymond M., Laser Remote Sensing. Wiley-Interscience, NewYork, 1984.
5. O'Brien, M.D., T.D. Stevens, and C.R. Philbrick, "Optical Extinction from Raman Lidar Measurements," Optical Instruments for Weather forecasting, SPIE Proceedings Vol. 2832, 45-52, 1996.
6. Melfi, S. H., J. D. Lawrence Jr., and M. P. McCormick, "Observation of Raman Scattering by Water Vapor in the Atmosphere," *Appl. Phys. Lett.*, 15, 295 – 297, 1969.
7. Cooney, J. A., "Comparisons of Water Vapor Profiles Obtained by Radiosonde and Laser Backscatter," *J. Appl. Meteor.*, 9, 182 – 184, 1970.
8. Esposito, Steven T., "Applications and Analysis of Raman Lidar Techniques for Measurements of Ozone and Water Vapor in the Troposphere," Master of Science Thesis for Penn State University, Department of Electrical Engineering, May, 1999.